One-Armed Spiral Waves in Galaxy Simulations with Counter-Rotating Stars

One-Armed Spiral Waves in Galaxy Simulations with Counter-Rotating Stars

Neil F. Comins, Department of Physics and Astronomy, Bennett Hall, University of Maine, Orono, ME 04469, galaxy@maine.maine.edu

Richard V. E. Lovelace, Department of Astronomy, Cornell University, Ithaca, NY, 14853, rvl1@cornell.edu

and

Thomas Zeltwanger & Peter Shorey, Department of Physics and Astronomy, Bennett Hall, University of Maine, Orono, ME 04469

Received _____; accepted _____

ABSTRACT

Motivated by observations of disk galaxies with counter-rotating stars, we have run two-dimensional, collisionless $N-$body simulations of disk galaxies with significant counter-rotating components. For all our simulations the initial value of Toomre's stability parameter was $Q = 1.1$. The percentage of counter-rotating particles ranges from 25% to 50%. A stationary one-arm spiral wave is observed to form in each run, persisting from a few to five rotation periods, measured at the half-mass radius. In one run, the spiral wave was initially a leading arm which subsequently transformed into a trailing arm. We also observed a change in spiral direction in the run initially containing equal numbers of particles orbiting in both directions. The results of our simulations support an interpretation of the one armed waves as due to the two stream instability.

Subject headings: gravitation—instabilities—galaxies: evolution—kinematics & dynamics—stars:kinematics

1. Introduction

Several disk galaxies have been observed to contain counterrotating stars, including NGC 3593 (Bertola et al. 1996); NGC 4138 (Jore, et al. 1996), (Thakar, et al., 1996); NGC 4550 (Rubin, et al. 1992) , (Rix et al. 1992); NGC 7217 (Merrifield & Kuijen 1994); and NGC 7331 (Prada, et al. 1996). The observed mass fraction in counterrotating stars is remarkably high, ranging from $\approx 20\%$ to $\approx 50\%$. Lovelace, Jore, and Haynes (1997) (hereafter LJH) developed a theory of the two-stream instability in flat counter-rotating galaxies. The basic instability is similar to that found in counterstreaming plasmas (e.g., Krall & Trivelpiece 1973). LJH made several predictions, most notably that the presence of stars orbiting in both directions around the disk should create a strong instability of the $m = 1$ (one-arm) spiral waves; that the $m = 1$ wave with the strongest amplification is usually the leading spiral arm with respect to the dominant component; and that the spiral wave is stationary when there are equal co- and counterrotating components. The two-stream instablity may have been observed in earlier computer simulations which found $m = 1$ spiral waves in counterrotating disks (Sellwood & Merritt 1994; Sellwood & Valluri 1997; Howard et al. 1997); however the characterization the instability was very limited and tightly wrapped spiral waves were not observed. It is of interest that $m = 1$ perturbations in spiral disks are rather common (Rix & Zaritsky 1995; Zaritsky & Rix 1997). In some cases these may arise from counterrotating material.

We present here the results of three runs of our GALAXY code (Schroeder & Comins 1989; Schroeder 1989; Shorey 1996), each with different fractions of the stars initially in counterrotating orbits. The runs had 25%, 37.5%, and 50% counterrotating particles. In the notation of LJH, this corresponds to runs with $\xi_* = 0.25$, 0.375, and 0.50, respectively. Each run had a total of 100,000 collisionless, equal-mass particles embedded in a halo containing 75% of the total mass of the system. This halo mass is used to help suppress

the ubiquitous $m = 2$ "bar-mode" instability. This particular halo mass fraction is chosen because it restricts the bar to the inner one-quarter of the disk for the run with all the particles moving in the same direction, while, along with the effect of the counterrotating particles, helping to completely suppress the bar in the $\xi_* = 0.50$ run (Kalnajs 1977). A halo mass fraction much larger than this severely limits the instability we are studying (Comins et al. 1997).

The simulation is done on a Cartesian grid with 256×256 cells. The radial mass distributions of both the particles and the halo are that described in Sellwood & Carlberg (1984) and Carlberg & Freedman (1985) for simulating the rotation curve of an Sc galaxy. The initial value of Toomre's (1964) stability parameter is $Q = 1.1$ over the entire disk. This Q increases due to heating throughout the run, bringing the disk to a Q consistent with the values in real galaxies. Toomre's critical radial wavenumber $k_{crit} = \kappa^2/(2\pi G\Sigma)$ satisfies the condition assumed by LJH for tightly wrapped spiral waves, $k_{crit}r \gg 1$, over all but the very center of the disk ($k_{crit}r$ varies from 7 at $0.1r_{max}$ to 15 at r_{max}). Here, κ is the epicyclic frequency and Σ is the total surface mass density. For our Galaxy, $k_{crit}r \approx 2\pi$ at the radius of the Sun (Binney & Tremaine 1987). The LJH theory predicts an e-folding time of about $1/\pi$ of a rotation period for $\xi_* = 0.5$ for a wave with radial wavenumber $(k_r) \approx 1.85k_{crit}$ and $Q = 1$. The e-folding time increases and the wavenumber decreases (to $(k_r) \approx 0.9k_{crit}$) as Q increases. There is no growth for $Q > 1.8$. Each run lasted 8 rotation periods, as measured at the half-mass radius of the disk. In §§$2 - 4$ we consider each run separately. In §5 we compare and contrast them and present our conclusions.

2. $\xi_* = 0.50$ Case

This run began with very little large$-m$ spiral development, compared to what occurs in the other cases we consider or when all the stars are orbiting in the same direction.

Indeed, the disk remains featureless for three-quarters of a rotation period. Theoretically, the $\xi_* = 0.50$ case (equal numbers of particles traveling in both directions) has no preferred direction of motion. However, the symmetry is broken by the Monte Carlo particle position and velocity loads. Initially there are 0.03% more particles moving clockwise in this run.

The initial, stationary spiral in this run points counterclockwise (Figure 1). Stationary here, and throughout this paper, means that the spiral structure rigidly rotates less than 10^o per rotation period. The spiral shown in Figure 1 became noticeable after 3/4 of a

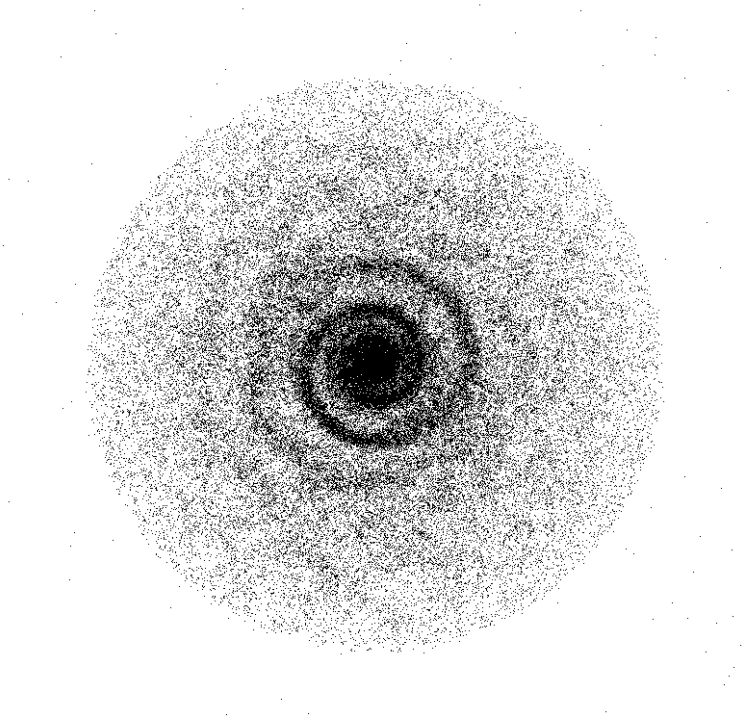

Fig. 1.— Leading, one-arm spiral concentrated in the inner regions of the $\xi_* = 0.50$ run at time $t = 1.75$ rotation periods, where the rotation period is measured at the half mass radius. This spiral developed after only 3/4 of a rotation period and persisted for 4 rotation periods. For all our runs, the radial mass distribution models an Sc galaxy; is 10^5; 75% of the gravitating mass is in an inert halo with the same radial mass distribution as the stars; the Cartesian grid is composed of 256×256 cells; and $Q_0 = 1.1$.

rotation period of the disk and it persisted for 4 rotation periods. During this time it was stationary and its linear growth had ceased, giving saturation of the mode amplitude. As defined in LJH, the initial growth rate $\omega_i \approx 0.14\Omega$ during the first rotation period is well below the maximum growth rate predicted by LJH of 0.5Ω. The spiral arm then changed direction, taking one rotation period (between the fifth and sixth rotation periods) to make the transition. This reversed spiral was also stationary and it persisted for about two rotation periods, by which time the disk also showed a series of spiral arcs. Figure 2 shows the reversed spiral. The $m = 1$ Fourier amplitude begins to decrease as soon as Q exceeded

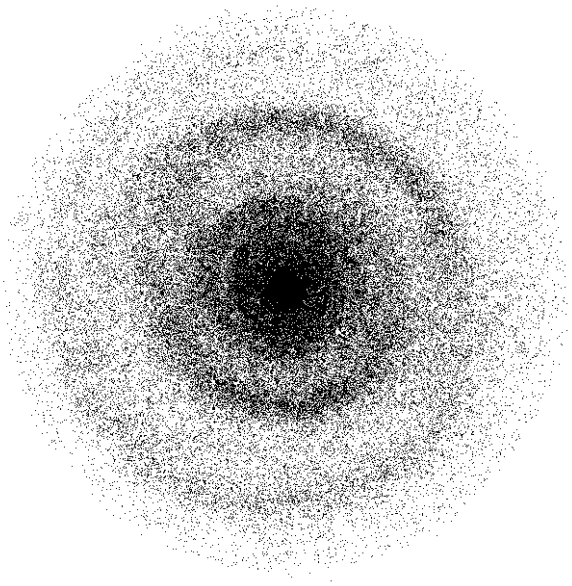

Fig. 2.— Trailing, one-arm spiral late in the $\xi_* = 0.50$ run at time $t = 6.5$ rotation periods. Note that unlike the earlier, leading-arm spiral shown in Figure 1, this spiral covers almost the entire disk.

1.8, as predicted by LJH. Figure 3 shows this effect.

3. $\xi_* = 0.375$ Case

This run begins with the development of weak multiarm spirals. Within one rotation period these are replaced by a stationary, leading, one-arm spiral that persists for about two rotation periods. This spiral is similar in appearance to the one in Figure 1, rotated by roughly 180 degrees. This spiral then transforms into a single trailing-arm spiral. The change occurs in a fraction of a rotation period. This spiral then splits into a combination of leading and trail-arm segments. Figure 4 shows the mix of leading and trailing arcs that constitute the stationary structure for five rotation periods late in the run. Once again, the $m = 1$ Fourier amplitude begins to decay when Q increases above 1.8.

4. $\xi_* = 0.25$ Case

This run begins with the formation of trailing multi-arm spirals within the first one quarter of a rotation period. These arms are numerous, relatively weak (Fourier amplitudes less than 0.003), and they are similar in appearance to those seen at the beginning of a typical run in which all particles are orbiting in the same direction ($\xi_* = 0$). The initial arms persist for over three rotation periods. During this time, an $m = 1$ trailing-arm spiral forms, eventually dominating the disk with a maximum Fourier amplitude of 0.10. The weaker multiple-arm structure vanishes. The one-arm spiral is stationary and it remains for about 4 rotation periods. It is less tightly wound than the spiral in Figure 1, but more tightly wound than the spiral in Figure 2. The $m = 1$ mode begins decreasing in Fourier amplitude as Q increases above 1.8, as predicted by LJH. As this $m = 1$ spiral fades, it is replaced with a small bar, which persists for the remainder of the run.

5. Discussion

Our simulations support many of the features of the "two-stream" instability in galactic disks with counterrotating stars, as presented in LJH. Consistent with the theory we see: one-armed spirals; decrease in the amplitude of this spiral as the Toomre Q of the system exceeds 1.8; strengthening of the spiral wave amplitude with ξ_* (for $\xi_* \leq 0.5$); and leading-arm spirals. The strength of the one-arm instability is predicted by LJH to be strongest in the $\xi_* = 0.50$ case, consistent with our simulation. Indeed, the Fourier amplitude A_1 of the arm there is 7 times greater than in the $\xi_* = 0.375$ case and 16 times greater than in the $\xi_* = 0.25$ case.

We do note some discrepencies between our results and the existing two-stream theory. First, the one-armed spiral in the $\xi_* = 0.25$ run developed and remained as a trailing-arm spiral. We attribute this to the particularly strong trailing, multiarm spirals that developed at the beginning of this run. We believe that the organized motion of the particles in the trailing arms damped the leading arm instability, and transferred energy to the more slowly amplifying, trailing, one-arm spiral. The influence of strong initial trailing-arm spiral growth and the resulting coupling between modes with different numbers of arms is not addressed in the two-stream instability theory as presented in LJH. Therefore, this result probably does not contradict the theory.

Sellwood and Merritt (1994) earlier found unstable $m = 1$ modes, but their work differs from the present paper by having $k_r r$ not large compared with unity and having the unstable modes localized in the inner part of the disk where $Q(r)$ was smallest and where the rotation curve was rising. Comparisons with Sellwood and Valluri (1997) and Howard et al. (1997) is not possible because they do not give $k_{crit}(r)$.

Finally, we observed dominant spirals changing direction, a phenomenon that is not predicted by the present version of the two-stream instability. Figure 5 shows that with

pattern speed $\Omega_p = 0$, the spiral encounters no resonances, making it possible for the wave to propagate through the center of the disk and thereby reverse direction.

For the $\xi_* = 0.375$ case, the leading arm spiral occurred only in the inner quarter of the disk's radius. The subsequent trailing arm extended over three quarters of the disk. This transformation appears to be consistent with the behaviour of a swing amplfier. We see precisely the same qualitative behaviour as depicted in Toomre (1981 Figure 8), where the leading spiral is only in the inner region of the disk. It then undergoes a transformation to a trailing arm spiral extending over a much larger radial extent. We are pursuing this issue of whether we are seeing swing amplification.

The strength and long lifetimes of the one-arm spiral waves, as shown by the runs presented here, suggests that there may be one-armed spiral features in galaxies with counterrotating components.

We are continuing to pursue this intriguing phenomenon in a variety of ways, including simulations with more particles (which will slow the rate of increase of Q), simulations using a gravitating gas component, simulations using other initial values of Q, and simulations using other initial radial mass distributions. In particular, we have found the one-arm spiral waves to persist for over ten rotation periods in a $Q_o = 1.1$, $\xi_* = 0.5$ Kuz'min disk. We are also developing a three dimensional code in which to explore mergers of counterrotating disks.

6. Acknowledgements

N.F.C. wishes to thank Sun Microsystems, Inc., for a grant of computers on which this work was done, and Bruce Elmegreen for a helpful discussion. The work of R.V.E.L. was supported in part by NSF grant AST 93-20068.

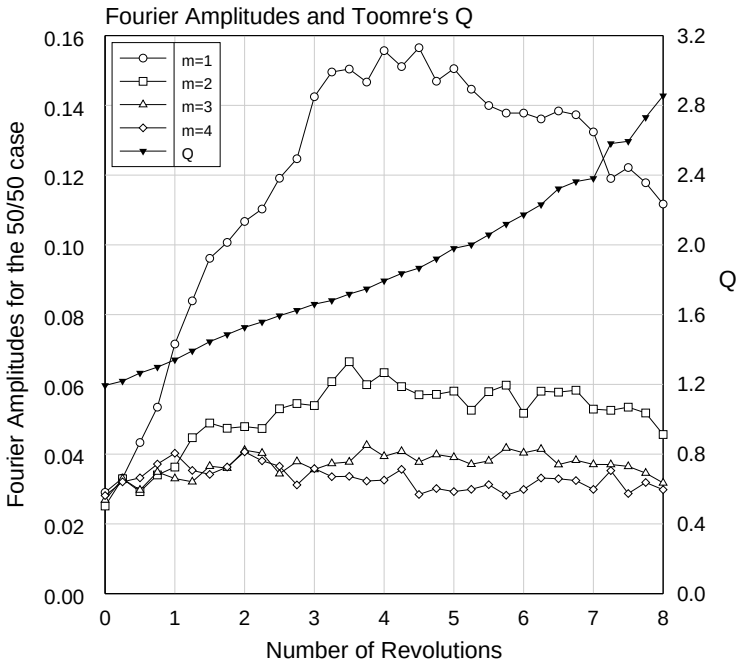

Fig. 3.— Azimuthal Fourier amplitudes and Toomre's Q for the $\xi_* = 0.50$ run. These results are averaged over the entire disk. Note the decrease in the $m = 1$ Fourier amplitude after Q increases beyond 1.8. The Fourier amplitudes are $A_m(t) = \sum_{j=0}^{95} \sum_{k=1}^{32} \Sigma_k(j,t) e^{2\pi i k m/32}$ where j indicates the annulus and $\Sigma_k(j,t)$ is the surface mass density in annulus j at angle $2\pi k/32$.

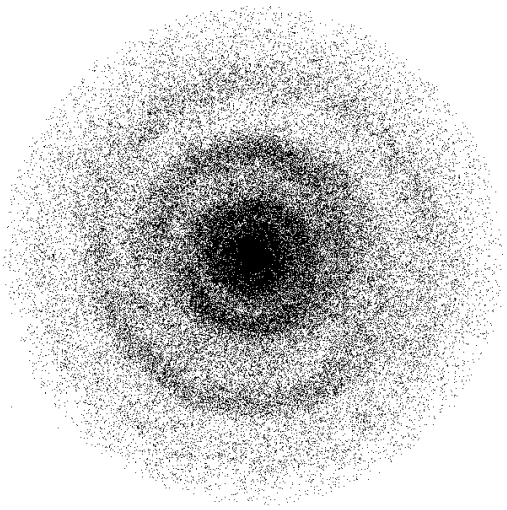

Fig. 4.— Arcs late in the $\xi_* = 0.375$ run, at time $t = 5$ rotation periods. These developed after the leading-arm spiral transformed into a trailing one-arm spiral during less than 1/4 of a rotation period. The trailing spiral fragmented into the arcs depicted here, which persisted for 5 rotation periods.

REFERENCES

Bertola, F., Cinzano, P., Corsini, E. M., Pizzella, A., Persic, M., & Salucci, P. 1996 ApJ, 458, L67

Binney, J.,& Tremaine, S. 1987, Galactic Dynamics (Princeton: Princeton Univ. Press)

Carlberg, R.G., & Freedman, W.L. 1985, ApJ, 298, 486

Comins, N.F., Zeltwanger, T., Lovelace, R.V.E., & Shorey, P.A. 1997, in preparation

Howard, S., Carini, M.T., Byrd, G.G., & Lester, S. 1997, AJ, in press

Jore, K.P., Broeils, A.H., & Haynes, M.P. 1996, submitted to AJ

Kalnajs, A.J. 1977, ApJ, 212, 637

Krall, N.A. & Trivelpiece, A.W., 1973, *Principles of Plasma Physics* (New York: McGraw Hill), ch. 9

Lovelace, R.V.E., Jore, K.P., & Haynes, M.P. 1997, ApJ, 475, 83

Merrifield, M.R., & Kuijken, K. 1994, ApJ, 432, 575

Prada, F., Gutierres, C.M., Peletier, R.F., & McKeith, C.D. ??? 1996, submitted to ApJ

Press, W.H., Flannery, B.P., Teukolsky, S.A., & Vetterling, W.T., 1986, *Numerical Recipes* (Cambridge: Cambridge University Press), ch. 12

Rix, H.W., Franx, M., Fisher, D., & Illingworth, G. 1992, ApJ, 400, L5

Rix, H.W., & Zaritsky, D. 1995, ApJ, 447, 82

Rubin, V., Graham, J.A., & Kenney, J.D.P. 1992, ApJ, 394, L9

Schroeder, M.C. 1989, Ph.D. Thesis, University of Maine

Schroeder, M.C., & Comins, N.F. 1989, ApJ, 346, 108

Sellwood, J.A., & Carlberg, R.G. 1984, ApJ, 282, 61

Sellwood, J.A., & Merritt, D. 1994, ApJ, 425, 530

Sellwood, J.A., & Valluri, M. 1997, MNRAS, in press

Shorey, P.A. 1996, Ph.D. Thesis, University of Maine

Thakar, A.R., Ryden, B.S., Jore, K.P., & Broelis, A.H. 1996, submitted to ApJ

Toomre, A. 1964, ApJ, 139, 1217

Toomre, A. 1981, in *The Large-Scale Structure of the Universe*, IAU Symposium No. 79, ed. M.S. Longair & J. Einasto, (Dordrecht: Reidel), p. 109

Zaritsky, D. & Rix, H.W. 1997, ApJ, submitted